Proceedings of the 3rd IFAC Workshop on Automatic Control in Offshore Oil and Gas Production, Esbjerg, Denmark, May 30 - June 1, 2018

We_C_Regular_Talk.1

Production Optimization of a Rigorous Thermal and Compositional Reservoir Flow Model[*]

Tobias K. S. Ritschel, **John Bagterp Jørgensen**

Department of Applied Mathematics and Computer Science &
Center for Energy Resources Engineering (CERE),
Technical University of Denmark, DK-2800 Kgs. Lyngby, Denmark

Abstract: We model thermal and compositional reservoir production as mass and energy balances combined with a phase equilibrium constraint. The phase equilibrium constraint is modeled as a thermodynamically rigorous UV flash process. The UV flash problem is a mathematical statement of the second law of thermodynamics, and it replaces the condition of equality of fugacities that is often used. We demonstrate that such a thermal and compositional reservoir model is in a semi-explicit index-1 differential-algebraic form, and we briefly describe a gradient-based single-shooting algorithm for the solution of production optimization problems. We implement the algorithm in C/C++ using the software DUNE, the thermodynamic software ThermoLib, and the optimization software KNITRO. We present an example of optimal water flooding where the injected water has a higher temperature than the reservoir fluid.

Keywords: Thermal and compositional model, Phase equilibrium, Optimal control

1. INTRODUCTION

Production optimization is concerned with maximizing a financial measure over the expected lifetime of an oil reservoir. It combines numerical simulation of the subsurface reservoir flow with numerical optimization. Production optimization is applicable to both traditional recovery methods, such as waterflooding, and to enhanced oil recovery methods such as chemical, biological, and thermal methods. The simulation and optimization of enhanced oil recovery processes often require compositional flow models. In particular, thermal recovery processes require thermal and compositional models.

Thermal and compositional reservoir flow models combine two main principles; 1) conservation of mass and energy, and 2) phase equilibrium. The phase equilibrium condition is based on a thermodynamic state function being minimal or maximal (Michelsen, 1999). The phase equilibrium condition is therefore formulated as a mathematical optimization problem, i.e. it is an optimization problem within the production optimization problem. The optimization problem that is relevant to thermal and compositional models is called the UVn flash problem because the internal energy, U, the volume, V, and the total amount of moles of each chemical species, n, are specified as parameters in the problem. The UVn flash is a mathematical formulation of the second law of thermodynamics which states that the entropy, S, of a closed system in equilibrium is maximal. This problem is often just called the UV flash because the total amount of moles are specified in all flash problems. It is also called the isochoric-isoenergetic flash. The solution to the UV flash problem is the equilibrium temperature,

pressure, and the phase compositions (in moles). The most commonly known flash problem is the PT flash problem where both temperature and pressure are specified and Gibbs energy is minimized. This is the problem that is most often encountered in the reservoir simulation and optimization literature. However, there it is formulated as the equality of fugacities and not as an optimization problem (Zaydullin et al., 2014; Kourounis et al., 2014). The condition of equal fugacities can be derived from the first-order optimality conditions of the PT flash problem. The PT flash is common because it can be solved efficiently with unconstrained optimization methods and because it is equivalent to other types of flash problems when it is combined with algebraic constraints on the specified quantities, e.g. the UV flash is equivalent to the combination of constraints on the internal energy, U, and the volume, V, and the PT flash. The UV flash is a key component in rigorous modeling of several vapor-liquid equilibrium processes such as fluid vessels and flash drums (Arendsen and Versteeg, 2009; Castier, 2010; Lima et al., 2008), distillation columns (Flatby et al., 1994), and two-phase computational fluid dynamical problems (Qiu et al., 2014; Hammer and Morin, 2014). Recently, a gradient-based single-shooting algorithm for the dynamic optimization of UV flash processes was developed by Ritschel et al. (2017a). The algorithm uses an adjoint method to compute gradients.

Most research in production optimization algorithms considers simple two-phase flow models that contain a water component and an oil pseudo-component. Some authors have solved production optimization problems involving polymer flooding (Lei et al., 2012). Such problems do not involve phase equilibrium conditions. More recently Kourounis et al. (2014) applied a gradient-based single-

shooting algorithm to a compositional model. Furthermore, Zaydullin et al. (2014) described a framework for fully thermal and compositional reservoir simulation. It is common to use single-shooting algorithms to solve production optimization problems (Bukshtynov et al., 2015; Kourounis et al., 2014; Forouzanfar et al., 2013; Capolei et al., 2012). Some authors have also used multiple-shooting (Codas et al., 2017; Capolei and Jørgensen, 2012) and simultaneous collocation (Heirung et al., 2011). These three methods belong to the class of gradient-based methods. There are two other classes of algorithms that authors use to solve production optimization problems; 1) gradient-free methods (Zhao et al., 2016) and 2) artificial intelligence methods (Onwunalu and Durlofsky, 2010; Saputelli et al., 2002). The advantage of gradient-based methods is that they are computationally efficient. The disadvantages of gradient-based methods are 1) that they require the computation of gradients which can be cumbersome for complex models, and 2) that they converge to local minima.

The novelty of this work is the rigorous modeling of thermal and compositional production optimization as a UV flash process. We describe the UV flash problem and the mass and energy conservation equations of the model. We implement the single-shooting algorithm described by Ritschel et al. (2017a) in C/C++ and provide an example of an optimal water injection strategy where the injected water has a higher temperature than the reservoir fluid.

Section 2 describes the thermal and compositional model, and Section 3 briefly describes the single-shooting algorithm. Section 4 provides a few details on the implementation, and Section 5 presents the numerical example. Section 6 presents conclusions.

2. RESERVOIR FLOW MODEL

In this section, we describe the thermal and compositional reservoir flow model and demonstrate that it is in the semi-explicit index-1 differential-algebraic form that is considered by Ritschel et al. (2017a). The model consists of a set of phase equilibrium conditions based on the second law of thermodynamics, a set of mass balance equations, and one energy balance equation. The phase equilibrium is reached at a much faster timescale than the flow processes and we therefore assume that the phases are in equilibrium at all times. The mass and energy conservation equations are based on models of advective fluid flow and thermal conduction in the rock.

2.1 Phase equilibrium

The fluid consists of water (w), oil (o), and gas (g). The oil and gas phases contain N_C chemical components. We assume that all fluid phases are in thermal, mechanical and chemical equilibrium with each other. We furthermore assume that the fluid is in thermal and mechanical equilibrium with the rock (r), i.e. $T = T^\alpha = T^r$ and $P = P^\alpha = P^r$ for $\alpha \in \{w, o, g\}$. We comment further on the thermal equilibrium between the fluid and the rock in Section 2.3. The phase equilibrium is governed by the UV flash in which the internal energy, U, the volume V, and the total amount of moles of each chemical species, n_w

and $n = [n_1; \ldots; n_{N_C}]$, are specified as parameters. The solution to the UV flash problem is the temperature, T, pressure, P, and phase composition vectors, n^w, n^o, and n^g, that maximize entropy under the above constraints:

$$\max_{T, P, n^w, n^o, n^g} \quad S^w + S^o + S^g + S^r, \tag{1a}$$

$$\text{subject to} \quad U^w + U^o + U^g + U^r = U, \tag{1b}$$

$$V^w + V^o + V^g + V^r = V, \tag{1c}$$

$$n^w = n_w, \tag{1d}$$

$$n_k^o + n_k^g = n_k, \quad k = 1, \ldots, N_C. \tag{1e}$$

The above optimization problem only contains equality constraints. The necessary first-order optimality conditions are therefore algebraic equations which are solved for each grid cell, simultaneously with the conservation equations, during simulation.

2.2 Mass conservation equations

The fluid flow process is advective. Each conservation equation contains a molar flux term and an injection/production source term:

$$\partial_t C_w = -\nabla \cdot \mathbf{N}^w + Q^w, \tag{2a}$$

$$\partial_t C_k = -\nabla \cdot \mathbf{N}_k + Q_k, \quad k = 1, \ldots, N_C. \tag{2b}$$

The molar component flux, $\mathbf{N}_k$, is

$$\mathbf{N}_k = x_k \mathbf{N}^o + y_k \mathbf{N}^g. \tag{3}$$

$\mathbf{N}^\alpha$ is the molar flux of phase $\alpha \in \{w, o, g\}$. x_k and y_k are oil and gas mole fractions. The molar injection/production terms are

$$Q^w = Q^{w,\text{inj}} - Q^{w,\text{prod}}, \tag{4a}$$

$$Q_k = - \left(x_k Q^{o,\text{prod}} + y_k Q^{g,\text{prod}} \right). \tag{4b}$$

Water is injected at a molar rate of $Q^{w,\text{inj}}$ while all fluid phases are produced at molar rates of $Q^{\alpha,\text{prod}}$.

2.3 Energy conservation equations

We first describe the energy conservation equations without assuming that the fluid and the rock are in thermal equilibrium. Then we describe how this assumption affects the model equations and present the model that assumes thermal equilibrium. The fluid (f) and rock (r) energy conservation equations are

$$\partial_t u^f = -\nabla \cdot \mathbf{N}_u^f + Q_u^f, \tag{5a}$$

$$\partial_t u^r = -\nabla \cdot \mathbf{N}_u^r + Q_u^r. \tag{5b}$$

u^f and u^r are internal energies per unit volume. The fluid heat flux is caused by advection of the phases:

$$\mathbf{N}_u^f = h^w \mathbf{N}^w + h^o \mathbf{N}^o + h^g \mathbf{N}^g. \tag{6}$$

h^α is the molar enthalpy of phase α. We model the conductive rock heat flux with Fourier's law of thermal conduction (Holman, 2010, Chap. 1):

$$\mathbf{N}_u^r = -k_T^r \nabla T^r. \tag{7}$$

k_T^r is the thermal conductivity of the rock. Both the wells and the conduction at the rock-fluid interface affect the fluid energy balance:

$$Q_u^f = h^{w,\text{inj}} Q^{w,\text{inj}} - \sum_{\alpha \in \{w, o, g\}} h^\alpha Q^{\alpha,\text{prod}} + Q^{rf}. \tag{8}$$

We model the thermal conduction at the rock-fluid interface with Newton's law of cooling (Holman, 2010, Chap. 1):

$$Q^{rf} = -k_T^{rf}(T^f - T^r). \tag{9}$$

T^f is the fluid temperature, and k_T^{rf} is the thermal conductivity of the rock-fluid interface. It is only the conduction at the rock-fluid interface that affects the rock energy balance:

$$Q_u^r = -Q^{rf}. \tag{10}$$

We now assume that the rock and the fluid are in thermal equilibrium. This corresponds to energy being transferred instantly through the rock-fluid interface, i.e. k_T^{rf} is infinite and $T = T^f = T^r$. We add (5a) and (5b) to obtain an energy conservation equation for the internal energy of the combined fluid-rock system, $u = u^f + u^r$:

$$\partial_t u = -\nabla \cdot \mathbf{N}_u + Q_u. \tag{11}$$

The combined heat flux and source terms are

$$\mathbf{N}_u = h^w \mathbf{N}^w + h^o \mathbf{N}^o + h^g \mathbf{N}^g - k_T^r \nabla T, \tag{12a}$$

$$Q_u = h^{w,\text{inj}} Q^{w,\text{inj}} - \sum_{\alpha \in \{w,o,g\}} h^\alpha Q^{\alpha,\text{prod}}. \tag{12b}$$

2.4 Darcy's law

The molar phase flux is the product of density and the volumetric phase flux, $\mathbf{N}^\alpha = \rho^\alpha \mathbf{u}^\alpha$. We describe the volumetric phase flux with Darcy's law:

$$\mathbf{u}^\alpha = -(k_r^\alpha/\mu^\alpha)\mathbf{K}\left(\nabla P - \rho^\alpha g \nabla z\right). \tag{13}$$

k_r^α is relative permeability, μ^α is viscosity, $\mathbf{K}$ is a permeability tensor, g is the gravity acceleration, and z is depth.

2.5 Well terms

The wells perforate certain grid cells in the discretized reservoir. The well models for these cells are

$$Q^{w,\text{inj}} = (1/V)\text{WI}\rho^w(k_r^w/\mu^w)(P^{\text{bhp}} - P), \tag{14a}$$

$$Q^{\alpha,\text{prod}} = (1/V)\text{WI}\rho^\alpha(k_r^\alpha/\mu^\alpha)(P - P^{\text{bhp}}). \tag{14b}$$

V is the volume of the perforated cell, WI is the well index, and P^{bhp} is the bottom-hole pressure in the well.

2.6 Relative permeabilities

We model the relative permeabilities with Stone's model II as described by Delshad and Pope (1989). The relative permeabilities are functions of the phase saturations, i.e. $k_r^\alpha = k_r^\alpha(\hat{S}^\alpha)$ where $\hat{S}^\alpha = V^\alpha/(V^w + V^o + V^g)$. The relative permeabilities are therefore functions of the temperature, pressure, and phase composition vectors:

$$k_r^\alpha = k_r^\alpha(T, P, n^w, n^o, n^g). \tag{15}$$

2.7 Viscosity

We use the phase viscosity model by Lohrenz et al. (1964). They describe the viscosity as a function of temperature, pressure, and phase composition, i.e.

$$\mu^\alpha = \mu^\alpha(T, P, n^\alpha). \tag{16}$$

2.8 Thermodynamics

We use a thermodynamical model by Ritschel et al. (2017b) to evaluate the enthalpy, entropy, and volumes of the fluid phases:

$$H^\alpha = H^\alpha(T, P, n^\alpha), \tag{17a}$$

$$S^\alpha = S^\alpha(T, P, n^\alpha), \tag{17b}$$

$$V^\alpha = V^\alpha(T, P, n^\alpha). \tag{17c}$$

We evaluate other thermodynamic functions with the fundamental thermodynamical relations $U = H - PV$, $G = H - TS$, and $A = U - TS$ (we only need U in this model).

2.9 Finite volume discretization

The conservation equations (2) and (11) are all in the form $\partial_t C = -\nabla \cdot \mathbf{N} + Q$. We integrate the equation over the i'th grid cell, Ω_i:

$$\partial_t \int_{\Omega_i} C \, dV = -\int_{\Omega_i} \nabla \cdot \mathbf{N} \, dV + \int_{\Omega_i} Q \, dV. \tag{18}$$

We apply Gauss' divergence theorem to the flux term and split up the resulting surface integral:

$$\int_{\Omega_i} \nabla \cdot \mathbf{N} \, dV = \int_{\partial\Omega_i} \mathbf{N} \cdot \mathbf{n} \, dA = \sum_{j \in \mathcal{N}^{(i)}} \int_{\gamma_{ij}} \mathbf{N} \cdot \mathbf{n} \, dA. \tag{19}$$

$\partial\Omega_i$ is the boundary of Ω_i, and γ_{ij} is the face shared by grid cell i and j. $\mathbf{n}_{ij}$ is the outward normal vector, and $\mathcal{N}^{(i)}$ is the set of cells that share a face with grid cell i. We evaluate the left-hand side integrals in (18) exactly:

$$U_i = \int_{\Omega_i} u \, dV, \tag{20a}$$

$$n_{w,i} = \int_{\Omega_i} C_w \, dV, \tag{20b}$$

$$n_{k,i} = \int_{\Omega_i} C_k \, dV. \tag{20c}$$

We approximate the remaining integrals with quadrature:

$$\int_{\Omega_i} Q \, dV \approx (QV)_i, \tag{21a}$$

$$\int_{\gamma_{ij}} \mathbf{N} \cdot \mathbf{n} \, dA \approx (A\mathbf{N} \cdot \mathbf{n})_{ij}. \tag{21b}$$

The right-hand side in (21b) contains gradients of T and P when applied to (2) and (11). We approximate these flux terms with a two-point flux approximation as described by Lie (2014). The resulting differential equations are

$$\dot{U}_i = \sum_{j \in \mathcal{N}^{(i)}} \left(\sum_{\alpha \in \{w,o,g\}} (h^\alpha \Gamma \hat{H}^\alpha \Delta\Phi^\alpha)_{ij} + (\Gamma_T \Delta T)_{ij} \right)$$
$$+ (Q_u V)_i, \tag{22a}$$

$$\dot{n}_{w,i} = \sum_{j \in \mathcal{N}^{(i)}} (\Gamma \hat{H}^w \Delta\Phi^w)_{ij} + (Q^w V)_i, \tag{22b}$$

$$\dot{n}_{k,i} = \sum_{j \in \mathcal{N}^{(i)}} (x_k \Gamma \hat{H}^o \Delta\Phi^o + y_k \Gamma \hat{H}^g \Delta\Phi^g)_{ij} + (Q_k V)_i. \tag{22c}$$

The term $(\Gamma \hat{H}^\alpha \Delta\Phi^\alpha)_{ij}$ approximates $-(A\mathbf{N}^\alpha \cdot \mathbf{n})_{ij}$. Γ_{ij} is the geometric part of the transmissibilities:

$$\Gamma_{ij} = A_{ij} \left(\hat{\Gamma}_{ij}^{-1} + \hat{\Gamma}_{ji}^{-1} \right)^{-1}, \tag{23a}$$

$$\hat{\Gamma}_{ij} = \left(\mathbf{K}_i \frac{c_{ij} - c_i}{|c_{ij} - c_i|^2} \right) \cdot \mathbf{n}_{ij}. \tag{23b}$$

A_{ij} is the area of γ_{ij}, c_{ij} is the center of γ_{ij}, and c_i is the center of Ω_i. $\hat{\Gamma}_{ij}$ is the one-sided transmissibility. We define $\Gamma_{T,ij}$ similar to Γ_{ij} where k_T^r replaces $\mathbf{K}$. The potential difference and the fluid part of the transmissibilities are

$$\Delta\Phi_{ij}^\alpha = (\Delta P - \rho^\alpha g \Delta z)_{ij}, \tag{24a}$$

$$\hat{H}_{ij}^\alpha = \begin{cases} (\rho^\alpha k_r^\alpha/\mu^\alpha)_i, & \Delta\Phi_{ij}^\alpha < 0, \\ (\rho^\alpha k_r^\alpha/\mu^\alpha)_j, & \Delta\Phi_{ij}^\alpha \geq 0, \end{cases} \tag{24b}$$

where $\Delta P_{ij} = P_j - P_i$, $\Delta z_{ij} = z_j - z_i$, and $\rho_{ij}^\alpha = 0.5(\rho_i^\alpha + \rho_j^\alpha)$. We have upwinded the fluid part of the transmissibilities, $\hat{H}^\alpha$, in order to ensure numerical stability. We upwind x_k, y_k, and h^α in the same way.

2.10 Differential-algebraic model

We introduce the state variables $x_i = [U; n_w; n]_i \in \mathbb{R}^{2+N_C}$, the algebraic variables $y_i = [T; P; n^w; n^o; n^g]_i \in \mathbb{R}^{3+2N_C}$, the manipulated input variables $u_i = P_i^{\text{bhp}} \in \mathbb{R}$, and the disturbance variables $d_i = T_i^{\text{inj}} \in \mathbb{R}$. T^{inj} is the temperature of the injected water used to evaluate $h^{w,\text{inj}}$ in (8). The UV flash problem (1) is thus in the form

$$\min_{y_i} \quad f(y_i), \tag{25a}$$

$$\text{s.t.} \quad g(y_i) = x_i, \tag{25b}$$

$$h(y_i) = 0. \tag{25c}$$

The optimality conditions of (25) are in the form $G_i(x_i, y_i, z_i)$ where $z_i \in \mathbb{R}^{3+N_C}$ are Lagrange multipliers (Ritschel et al., 2017a). We enforce the phase equilibrium in each grid cell. The left-hand side of the differential equations (22) contains derivatives of the state variables, x_i, and all quantities on the right-hand side depend on the algebraic variables, y_i, the manipulated inputs, u_i, or the disturbance variables, d_i. The differential equations (22) are therefore in the form $\dot{x}_i(t) = F(y_i(t), u_i(t), d_i(t))$, and the discretized reservoir flow model is in the form

$$G(x(t), y(t), z(t)) = 0, \tag{26a}$$

$$\dot{x}(t) = F(y(t), u(t), d(t)), \tag{26b}$$

where G is the phase equilibrium conditions for all cells, and F is the spatially discretized right-hand side of the flow equations for all cells.

3. PRODUCTION OPTIMIZATION

In this section, we briefly describe the gradient-based single-shooting algorithm by Ritschel et al. (2017a). The production optimization problem is in the form

$$\min_{[x(t);y(t);z(t)]_{t_0}^{t_f}, \{u_k\}_{k\in\mathcal{N}}} \phi = \int_{t_0}^{t_f} \Phi(y(t), u(t), d(t))dt, \tag{27a}$$

subject to

$$x(t_0) = \hat{x}_0, \tag{27b}$$

$$G(x(t), y(t), z(t)) = 0, \quad t \in \mathcal{T}, \tag{27c}$$

$$\dot{x}(t) = F(y(t), u(t), d(t)), \ t \in \mathcal{T}, \tag{27d}$$

$$u(t) = u_k, \ t \in [t_k, t_{k+1}[, \quad k \in \mathcal{N}, \tag{27e}$$

$$d(t) = \hat{d}_k, \ t \in [t_k, t_{k+1}[, \quad k \in \mathcal{N}, \tag{27f}$$

$$\{u_k\}_{k\in\mathcal{N}} \in \mathcal{U}. \tag{27g}$$

The objective function, ϕ in (27a), is a financial measure, e.g. total oil production or net present value, (27b) is an initial condition on the state variables, (27c)-(27d) are the equilibrium conditions and the spatially discretized reservoir flow equations, and (27e)-(27f) are zero-order

hold parametrizations of the manipulated inputs and disturbance variables. Finally, (27g) are constraints on the manipulated inputs, typically linear or bound constraints. $\mathcal{T} = [t_0, t_f]$ is the time interval, and $\mathcal{N} = \{0, \ldots, N-1\}$ is the set of timestep indices. N is the number of timesteps.

3.1 Numerical simulation

For simplicity, we describe the algorithm with the assumption that the timesteps coincide with the control intervals. The actual implementation uses an ESDIRK12 method with a simplified version of the stepsize controller described by Völcker et al. (2010). The differential equations are discretized with Euler's implicit method. That results in the nonlinear residual equations $R_{k+1} = 0$ where

$$R_{k+1} = \begin{bmatrix} x_{k+1} - x_k - \Delta t_k F(y_{k+1}, u_k, \hat{d}_k) \\ G(x_{k+1}, y_{k+1}, z_{k+1}) \end{bmatrix}, \tag{28}$$

for $k \in \mathcal{N}$. We introduce $w = [x; y; z]$ and solve the nonlinear equations with Newton's method:

$$w_{k+1}^{m+1} = w_{k+1}^m - (\partial R_{k+1}/\partial w_{k+1})^{-1} R_{k+1}(w_{k+1}^m). \tag{29}$$

We use an ILU preconditioned GMRES method to solve the linear system in (29).

3.2 The single-shooting algorithm

In the single-shooting approach, we transcribe the infinite-dimensional optimal control problem (27) into the following finite-dimensional optimization problem

$$\min_{\{u_k\}_{k\in\mathcal{N}}} \quad \psi = \psi\left(\{u_k\}_{k\in\mathcal{N}}; \hat{x}_0, \{\hat{d}_k\}_{k\in\mathcal{N}}\right), \tag{30a}$$

$$\text{subject to} \quad \{u_k\}_{k\in\mathcal{N}} \in \mathcal{U}, \tag{30b}$$

where the objective function is

$$\psi = \left\{ \phi = \sum_{k\in\mathcal{N}} \Phi_k(y_{k+1}, u_k, \hat{d}_k) : \tag{31a} \right.$$

$$x_0 = \hat{x}_0, \tag{31b}$$

$$\left. R_{k+1}(w_{k+1}; x_k, u_k, \hat{d}_k) = 0, \ k \in \mathcal{N} \right\}, \tag{31c}$$

and $\Phi_k(y_{k+1}, u_k, \hat{d}_k) = \Delta t_k \Phi(y_{k+1}, u_k, \hat{d}_k)$. Efficient algorithms for the solution of the optimization problem (30) require the gradients of ψ, $\{\nabla_{u_k}\psi\}_{k\in\mathcal{N}}$. We use a discrete adjoint method to compute these gradients. We solve the following adjoint equations for the adjoints, $\{\lambda_{k+1}\}_{k\in\mathcal{N}}$, with an ILU preconditioned GMRES method:

$$(\partial R_N/\partial w_N)^T \lambda_N = -\nabla_{w_N}\Phi_{N-1}, \tag{32a}$$

$$(\partial R_k/\partial w_k)^T \lambda_k = -(\partial R_{k+1}/\partial w_k)^T \lambda_{k+1} - \nabla_{w_k}\Phi_{k-1}. \tag{32b}$$

The adjoint equations are solved in a backwards manner starting with (32a) and proceeding with (32b) for $k = N-1, N-2, \ldots, 1$. The gradients of ψ are computed with

$$\nabla_{u_k}\psi = \nabla_{u_k}\Phi_k + (\partial R_{k+1}/\partial u_k)^T \lambda_{k+1}, \quad k\in\mathcal{N}. \tag{33}$$

4. IMPLEMENTATION

We implement the single-shooting algorithm in C++. We use the DUNE software to solve linear systems with iterative methods (Blatt and Bastian, 2007) and for grid management (Bastian et al., 2008). We use C routines
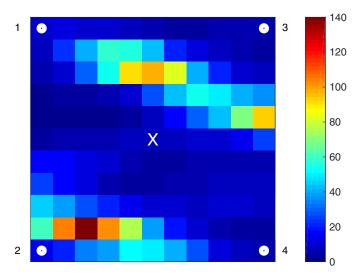
Fig. 1. Permeability field [mD]. A white circle indicates an injector, and the white X indicates the producer.

from the open-source software ThermoLib (Ritschel et al., 2017b, 2016) to evaluate thermodynamic functions. We use the optimization software KNITRO 10.2 to solve the optimization problem (30).

5. NUMERICAL EXAMPLE

In this section, we present a numerical example where four injectors inject water at $40°C$ into a $110 \times 110 \times 10$ m reservoir that contains a fluid at $20°C$. The oil and gas phases consist of methane, ethane, propane, n-heptane, and hydrogen sulfide. The reservoir is discretized with $11 \times 11 \times 1$ cells. The objective is to maximize the oil production. The wells are placed in a five spot pattern as shown in Fig. 1 which also shows the permeability field. The producer bottom-hole pressure (BHP) must be in the interval [10 MPa, 11 MPa] and the injector BHPs must be in [11 MPa, 12 MPa]. The optimal production strategy is shown in Fig. 2 together with the cumulative oil and gas production. Fig. 2 also shows (in dashed lines) the oil and gas production for a maximum injection strategy with maximum injector BHP and minimum producer BHP. The optimal oil production is 35% higher than what is obtained with the maximum injection strategy while the gas production is lower.

6. CONCLUSIONS

In this work, we present a fully thermal and compositional reservoir flow model based on a rigorous formulation of the phase equilibrium using the second law of thermodynamics, i.e. the entropy of a closed system in equilibrium is maximal. This results in an inner optimization problem called the UV flash problem. The reservoir flow model is in the semi-explicit index-1 differential-algebraic form that Ritschel et al. (2017a) consider, and we implement their gradient-based single-shooting algorithm for production optimization. We present a numerical example where the injected water has a higher temperature than the reservoir fluid. Future work will involve isothermal compositional models based on the model presented in this work.
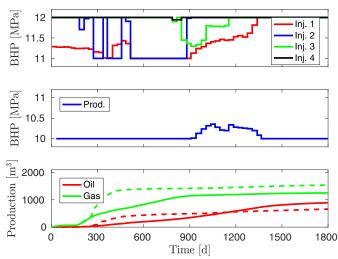

Fig. 2. Optimal well BHPs and oil and gas production (solid: optimal strategy, dashed: reference strategy).

REFERENCES

Arendsen, A.R.J. and Versteeg, G.F. (2009). Dynamic thermodynamics with internal energy, volume, and amount of moles as states: Application to liquefied gas tank. *Ind. Eng. Chem. Res.*, 48(6), 3167–3176.

Bastian, P., Blatt, M., Dedner, A., Engwer, C., Klöfkorn, R., Ohlberger, M., and Sander, O. (2008). A generic grid interface for parallel and adaptive scientific computing. Part I: Abstract framework. *Computing*, 82(2-3), 103–119.

Blatt, M. and Bastian, P. (2007). The iterative solver template library. In B. Kågström et al. (ed.), *Applied Parallel Computing. State of the Art in Scientific Computing. PARA 2006*, volume 4699 of *Lecture Notes in Computer Science*. Springer, Berlin, Heidelberg.

Bukshtynov, V., Volkov, O., Durlofsky, L.J., and Aziz, K. (2015). Comprehensive framework for gradient-based optimization in closed-loop reservoir management. *Comput. Geosci.*, 19(4), 877–897.

Capolei, A. and Jørgensen, J.B. (2012). Solution of constrained optimal control problems using multiple shooting and ESDIRK methods. In *Proceedings of the 2012 American Control Conference*, 295–300.

Capolei, A., Völcker, C., Frydendall, J., and Jørgensen, J.B. (2012). Oil reservoir production optimization using single shooting and ESDIRK methods. In *Automatic Control in Offshore Oil and Gas Production*, 286–291. International Federation of Automatic Control.

Castier, M. (2010). Dynamic simulation of fluids in vessels via entropy maximization. *J. Ind. Eng. Chem.*, 16(1), 122–129.

Codas, A., Hanssen, K.G., Foss, B., Capolei, A., and Jørgensen, J.B. (2017). Multiple shooting applied to robust reservoir control optimization including output constraints on coherent risk measures. *Comput. Geosci.*, 21(3), 479–497.

Delshad, M. and Pope, G.A. (1989). Comparison of the three-phase oil relative permeability models. *Transp. Porous Media*, 4(1), 59–83.

Flatby, P., Skogestad, S., and Lundström, P. (1994). Rigorous dynamic simulation of distillation columns based on UV-flash. In *IFAC Symposium on Advanced Control*
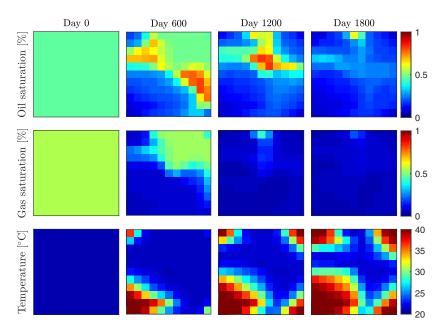
Fig. 3. Oil saturation, gas saturation, and temperature for the optimal oil production strategy.

of Chemical Processes (ADCHEM '94), 261–266.

Forouzanfar, F., Rossa, E.D., Russo, R., and Reynolds, A.C. (2013). Life-cycle production optimization of an oil field with an adjoint-based gradient approach. *J. Pet. Sci. Eng.*, 112, 351–358.

Hammer, M. and Morin, A. (2014). A method for simulating two-phase pipe flow with real equations of state. *Comput. Fluids*, 100, 45–58.

Heirung, T.A.N., Wartmann, M.R., Jansen, J.D., Ydstie, B.E., and Foss, B.A. (2011). Optimization of the waterflooding process in a small 2D horizontal oil reservoir by direct transcription. In *Proceedings of the 18th World Congress*, 10863–10868. International Federation of Automatic Control, Milano, Italy.

Holman, J.P. (2010). *Heat Transfer*. McGraw-Hill, 10th edition.

Kourounis, D., Durlofsky, L.J., Jansen, J.D., and Aziz, K. (2014). Adjoint formulation and constraint handling for gradient-based optimization of compositional reservoir flow. *Comput. Geosci.*, 18(2), 117–137.

Lei, Y., Li, S., Zhang, X., Zhang, Q., and Guo, L. (2012). Optimal control of polymer flooding based on maximum principle. *J. Appl. Math.*

Lie, K.A. (2014). *An Introduction to Reservoir Simulation Using MATLAB*. Sintef ICT, Oslo, Norway.

Lima, E.R.A., Castier, M., and Biscaia Jr., E.C. (2008). Differential-algebraic approach to dynamic simulations of flash drums with rigorous evaluation of physical properties. *Oil Gas Sci. Technol. Rev. IFP*, 63(5), 677–686.

Lohrenz, J., Bray, B.G., and Clark, C.R. (1964). Calculating viscosities of reservoir fluids from their compositions. *J. Pet. Technol.*, 16(10), 1171–1176.

Michelsen, M.L. (1999). State function based flash specifications. *Fluid Phase Equilib.*, 158-160, 617–626.

Onwunalu, J.E. and Durlofsky, L.J. (2010). Application of a particle swarm optimization algorithm for determining optimum well location and type. *Comput. Geosci.*, 14(1), 183–198.

Qiu, L., Wang, Y., and Reitz, R.D. (2014). Multiphase dynamic flash simulations using entropy maximization and application to compressible flow with phase change. *AIChE J.*, 60(8), 3013–3024.

Ritschel, T.K.S., Capolei, A., Gaspar, J., and Jørgensen, J.B. (2017a). An algorithm for gradient-based dynamic optimization of UV-flash processes. *Comput. Chem. Eng.* Accepted.

Ritschel, T.K.S., Gaspar, J., and Jørgensen, J.B. (2017b). A thermodynamic library for simulation and optimization of dynamic processes. In *Proceedings of the 20th World Congress of the International Federation of Automatic Control*.

Ritschel, T.K.S., Gaspar, J., Capolei, A., and Jørgensen, J.B. (2016). An open-source thermodynamic software library. Technical Report DTU Compute Technical Report-2016-12, Department of Applied Mathematics and Computer Science, Technical University of Denmark.

Saputelli, L., Malki, H., Canelon, J., and Nikolaou, M. (2002). A critical overview of artificial neural network applications in the context of continuous oil field optimization. In *SPE Annual Technical Conference and Exhibition*. Society of Petroleum Engineers, San Antonio, Texas.

Völcker, C., Jørgensen, J.B., Thomsen, P.G., and Stenby, E.H. (2010). Explicit singly diagonally implicit Runge-Kutta methods and adaptive stepsize control for reservoir simulation. In *Proceedings of the 12th European Conference on the Mathematics of Oil Recovery*. Oxford, UK.

Zaydullin, R., Voskov, D.V., James, S.C., Henley, H., and Lucia, A. (2014). Fully compositional and thermal reservoir simulation. *Comput. Chem. Eng.*, 63, 51–65.

Zhao, H., Tang, Y.W., Li, Y., Shi, Y.B., Cao, L., Gong, R.X., and Shang, G.H. (2016). Reservoir production optimization using general stochastic approximate algorithm under the mixed-linear-nonlinear constraints. *J Residuals Sci. Technol.*, 13(8).